Hydrogen treated, cap-opened Si nanotubes array anode for high power lithium ion battery

CrossMark

Jaehwan Ha [a], Ungyu Paik [a,b,*]

[a] Department of Materials Science & Engineering, Hanyang University, Seoul 133-791, Republic of Korea
[b] WCU Department of Energy Engineering, Hanyang University, Seoul 133-791, Republic of Korea

HIGHLIGHTS

► The anode electrode employs sealed Si nanotubes and opened Si nanotubes array.
► We improve the rate capability using simple modification of nanostructure.
► The rate capability of modified Si nanotubes is increased 15% at 1C than sealed Si nanotube.
► The system provides a significant new insight into designing high power anode materials.

ARTICLE INFO

ABSTRACT

Silicon is a promising anode material for lithium ion batteries due to its low discharge potential and high theoretical capacity. However, rapid capacity fading caused by large volume change during cycling and poor rate capability came from low lithium ion diffusivity limit its practical use. Here, we report a novel approach to provide higher accessibility of lithium ions to the Si surface and shorter lithium ion diffusion length in Si nanotube structures. Its tubular geometry and large surface area enable effective accommodation of large volume change and large lithium ion flux at the interface between Si and electrolyte, respectively. Hydrogen treated, cap-opened Si nanotubes electrode shows excellent rate capability. The proposed electrode geometry provides a significant new insight into designing high power anode materials for the advanced lithium ion batteries.

© 2012 Elsevier B.V. All rights reserved.

1. Introduction

Alloy type anode materials such as silicon, germanium and tin have recently received great attention due to their high theoretical lithium-storage capacities [1–4]. Among them, Si is the most promising candidate due to its high theoretical capacity (4200 mAh g^{-1}), which is ten times higher than that of graphite, and low discharge charge potential [5]. However, its practical use has been limited by poor cycle performance owing to the loss of electrical contact between the active material and the current collector resulting from large volumetric changes during cycling. Various approaches have been widely studied to overcome this problem using nanophase Si structures, including nanocrystals,

porous nanoparticles [6], nanowires [3,7] and nanotubes [1]. In the previous study, Song et al. demonstrated that the sealed Si nanotubes array is a desirable architecture for accommodating large volume change associated with lithium and achieving reversible behavior in morphological change, which lead to improvement in cycle retention and reliable operation of the battery [1]. Although significant advance in cyclability and structural stability of Si based anode has been achieved by designing electrode configuration, these Si systems do not meet high-power-rate property due to its inherently low electron conductivity and ion diffusivity [8]. While many efforts have been devoted on the improvement of the cyclability of Si based electrodes, the study on the improvement of rate capability has received little attention. However, the balanced electrode design in both energy density and high power density is crucial for critical applications such as large scale storage of renewable power sources, electric vehicle as well as mobile energy storage.

Here, we report on synthesis of cap-opened Si nanotubes array and its application as high power anode material for lithium ion

* Corresponding author. WCU Department of Energy Engineering, Hanyang University, Seoul 133-791, Republic of Korea. Tel.: +82 2 2220 0502; fax: +82 2 2281 0502.
E-mail address: upaik@hanyang.ac.kr (U. Paik).

batteries. The rate capability of the electrode is dominantly determined by both the electronic conductivity and the lithium ion diffusivity in the electrode. Si nanotubes array was directly grown on the current collector, which allows faster electron injection from current collector to active material and an efficient electron transport has been achieved along its one dimensional geometry. By removing the sealed cap, the diffusion length of lithium ion can be minimized. Furthermore, lithium ion flux can be significantly increased due to large interface area between the electrolyte and the active material since the inner surfaces of Si nanotubes is also overlaid with the electrolyte. This electrode configuration engineering enables enhancing lithium related kinetics, which leads to improvement in rate capability of electrode.

2. Experimental

2.1. Synthesis of nanostructure

The cap-opened Si nanotubes were prepared by cap-opening of sealed Si nanotube using a reactive ion etching (RIE) technique. The preparation of the "sealed" Si nanotube is described in our previous paper [1]. Briefly, Si thin layer was deposited on a sacrificial ZnO nanorod template by chemical vapor deposition (CVD) process and the template were etched away by thermal reduction process. For the preparation of the ZnO nanorod template, ZnO seed layer with a thickness of 200 nm was deposited on a stainless steel substrate (thickness: 15 μm, Nilaco, Tokyo, Japan) using a metal-organic CVD technique. The substrate temperature was 400 °C. Then the substrate with ZnO seed layer was transferred to a bath containing a precursor solution of 0.02 M zinc nitrate hexahydrate and 0.25 M hexamethylene tetramine. The growth of ZnO nanorods was carried out at 90 °C for 24 h in an oven. The precursor solution was periodically replaced (every 3 h) with a fresh solution to increase the length of ZnO nanorods. A Si shell layer was coated on the vertically aligned ZnO nanorods by a CVD process. Conformal deposition of Si was achieved at 540 °C with H_2 and SiH_4 (10% diluted in H_2) with flow rates of 10−30 and 50−70 sccm, respectively. Si shells were coated for 10 min growth. After the Si deposition, the sacrificial template of ZnO nanorods was selectively etched via a reduction process at 600 °C for 24 h under hydrogen atmosphere.

2.2. Modification of nanostructure

The cap of the "sealed" Si nanotubes was etched using RIE equipment (RIE 80 plus, Oxford Instrument) with chlorine plasma (chlorine 80 sccm, 80 mTorr, RF 150 W). The etching rate for Si was found to be ~60 nm min^{-1}. The etching was carried out for 50 s. Plasma etching of Si in chlorine plasma is a well-established technique [9−11]. However, chlorine plasma etching produces silicon chlorine compounds such as $SiCl$, $SiCl_2$, $SiCl_3$, and $SiCl_4$ on the Si surface [12,13]. In order to remove the compounds, the cap-opened Si nanotube was thermally treated at 600 °C for 24 h under hydrogen atmosphere [14]. Fig. S1 shows the schematic illustration for the synthesis process of three types of Si nanotubes arrays.

2.3. Evaluation of electrochemical performance

The electrochemical properties of Si nanotubes-based anode were investigated using coin-type half cells (2016R type). Si nanotubes directly grown on stainless steel substrate were used as a working electrode. Pure lithium metal foil was used as both reference and counter electrodes. 1.3 M $LiPF_6$ solution in a mixture of ethylene carbonate and diethylene carbonate (ED/DEC, 3:7 vol%, PANAX ETEC, Seoul, Korea) was used as an electrolyte. The mass of the synthesized vertically aligned Si tubular structure was

266.4 ± 6.2 μg cm^{-2}, which was measured using a microbalance (Sartorius SE2, resolution 1 μg, Sartorius, Goettingen, Germany) before and after the Si deposition process. The cells were galvanostatically charged and discharged in a voltage range from 0.01 V to 2 V versus Li/Li$^+$ at various current densities using a battery cycle tester TOSCAT 3000 (Toyo Systems, Tokyo, Japan).
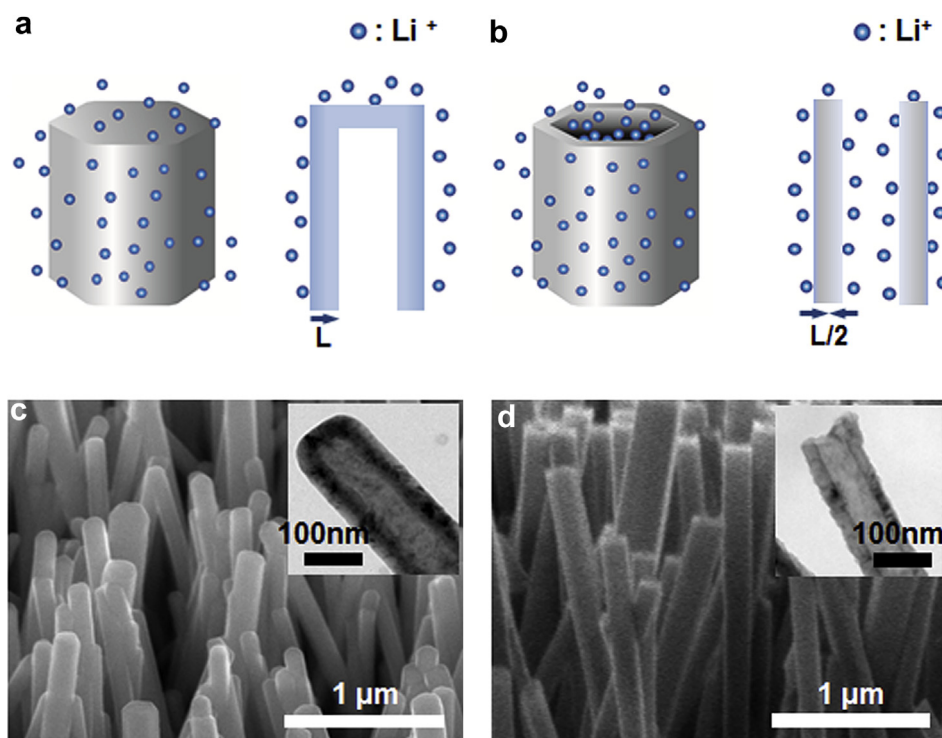
2.4. Material characterization

The structural information of Si nanotubes was obtained using a field emission scanning electron microscope (FE-SEM, JSM 4700F, JEOL, Japan) and a field emission transmission electron microscope (FE-TEM, JEM 2100F, JEOL, Japan). The compositional change in Si nanotubes was analyzed using an X-ray photoelectron spectroscopy (XPS, VG Multilab ESCA 2000).

3. Results and discussions

Schematic illustrations of sealed Si nanotubes and cap-opened Si nanotubes are shown in Fig. 1(a) and (b). The dimension of sealed Si nanotube and cap-opened Si nanotube is identical, and only difference between both the nanostructures is the morphology at the top region. Lithium ion diffusion length of cap-opened Si nanotubes is reduced to half of that of the sealed Si nanotubes since the lithium insertion is available via both inner and outer surfaces. Sealed Si nanotubes array and hydrogen treated, cap-opened Si nanotubes array have surface areas of 32.37 m^2 g^{-1} and 55.38 m^2 g^{-1}, respectively. Hydrogen treated, cap-opened Si nanotubes array has about 1.7 folds higher surface area compared to that of the sealed Si nanotubes array. These opened Si nanotube structure provides much higher interfacial area between active material and electrolyte, which increases the lithium ion flux from the electrolyte to active materials. The shorter lithium ion diffusion length and increased lithium ion flux enable the fast charge/discharge performance of the electrode [15]. Fig. 1(c) and (d) provides the electron microscope image of sealed Si nanotubes and cap-opened Si nanotubes, respectively. Both Si nanotube structures have a wall thickness of ~30 nm, inner diameter of ~60 nm. Top view scanning electron microscopy (SEM) images clearly confirmed that sealed cap was completely removed by reactive ion etching technique (RIE). Insets of Fig. 1(c) and (d) show transmission electron microscope images of sealed Si nanotubes and cap-opened Si nanotubes, respectively.

Fig. 2 shows the detailed morphological changes of Si nanotubes at each processing steps. The sealed Si nanotubes has a smooth wall surface and native oxide layer with a thickness of ~1 nm as shown in Fig. 2(a). After RIE process, the smooth wall surface became rough (Fig. 2(b)). This damage on the surface of cap-opened Si nanotubes was attributed to the etching plasma induced on the free space between Si nanotubes. During the etching process using chlorine as a reactive ion, silicon chloride compounds such as $SiCl$, $SiCl_2$, $SiCl_3$, and $SiCl_4$ could be formed on Si surface by the chemical reaction between unstable Si and Cl ion [12,13]. These chloride compounds form lithium chlorides by the reaction with lithium ions. The resulting lithium chlorides hinder the diffusion of lithium ions from the electrolyte into the active material [16,17]. Therefore, the chloride contaminations on the surface of Si nanotubes should be removed to improve the electrochemical performance. These chlorinated compounds can be removed by thermal treatment under hydrogen atmosphere. Thus, the cap-opened Si nanotubes were treated at 600 °C for 24 h under hydrogen atmosphere (hereinafter, referred as the hydrogen treated, cap-opened Si nanotubes) [14]. The rough surface was maintained after thermal treatment under hydrogen atmosphere. Both processes of cap-opening and thermal treatment under hydrogen atmosphere

Fig. 1. Schematic illustrations of (a) sealed Si nanotubes and (b) opened Si nanotubes and favorable lithium ion diffusion. SEM and TEM (insets) images of (c) sealed Si nanotubes and (d) opened Si nanotubes.
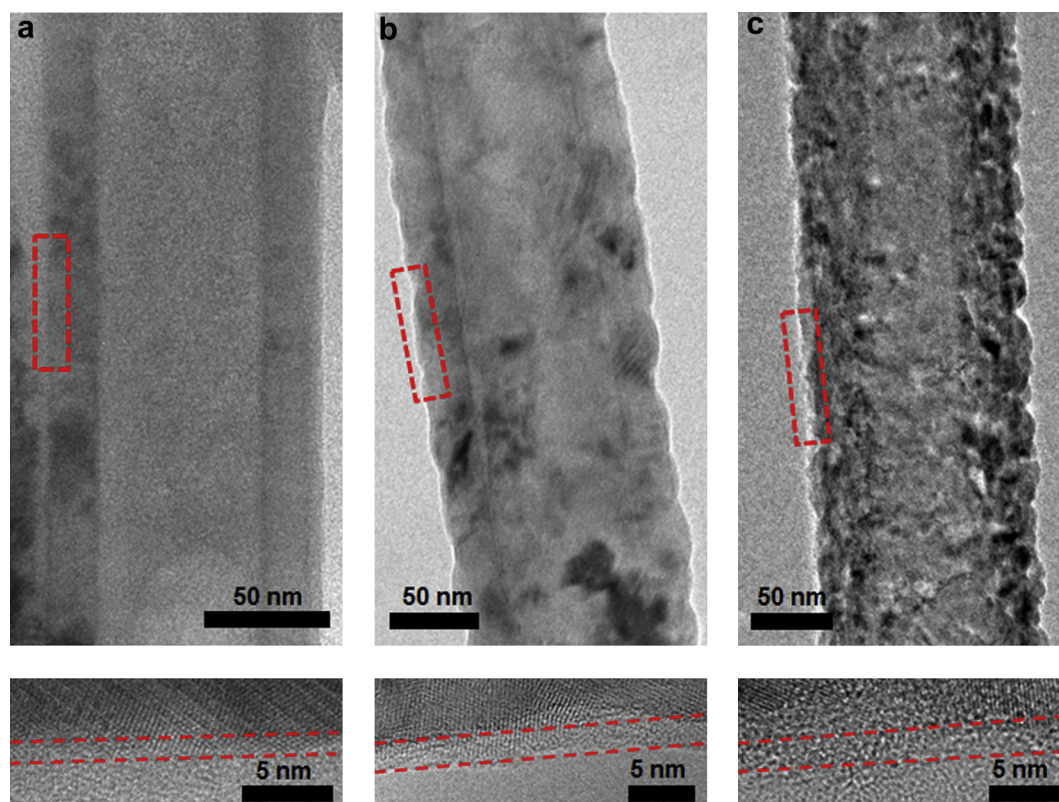
Fig. 2. Structural characterization of (a) sealed Si nanotubes, (b) cap-opened Si nanotubes, and (c) hydrogen treated, cap-opened Si nanotubes.

affected the structure of surface native oxide on Si. After both processes, the thickness of the oxide layer increases up to ~2.5 nm (Fig. 2(b) and (c)).

The Surface chemical state of Si nanotubes before and after the RIE and heat treatment processes was investigated by X-ray photoelectron spectroscopy (XPS). Fig. 3(a) shows the Si 2p XPS spectra of the sealed Si nanotubes. Two noticeable peaks were observed at 99.3 and 103.3 eV. These peaks can be assigned to metallic Si (Si^0) and SiO_2 (Si^{4+}), respectively [18]. After RIE process, the peak intensity for metallic Si decreases, whereas SiO_2 peak shows a significant increase [19]. For both sealed Si nanotubes and cap-opened Si nanotubes, a valley region between the 99.3 and 103.3 eV peaks indicates the presence of Si atoms with intermediate oxidation states (Si^{1+} to Si^{3+}). The valley observed for the sealed Si nanotubes can be attributed to the presence of SiO_x with different oxidation state. As the peaks of SiO_x and silicon chloride falls in the same region, it is not possible to distinguish the existence of silicon chloride compounds from SiO_x based on the Si 2p XPS spectra [20]. In order to analyze the presence of silicon chlorine compounds, Cl 2p XPS spectra were collected as shown in Fig. 3(d). It clearly shows the presence of chloride in the spectrum of cap-opened Si nanotubes after RIE process using chlorine plasma.

After the thermal treatment at 600 °C, the Cl 2p peak clearly disappeared (Fig. 3(d)), which indicates that the hydrogen thermal treatment is effective on removing the surface chloride compounds. The tail observed at the binding energy of about 105—108 eV in Fig. 3(b) and (c) can be attributed to the formation of silanol (Si—OH) [21]. The presence of silanol on the Si nanotubes was confirmed by O 1s XPS spectra (Fig. 3(e)). A tail at higher binding energy (up to ~ 537 eV) indicates the presence of silanol [22]. The origin of silanol on the cap-opened Si nanotubes after RIE process can be produced as a result of $SiCl_x$ reaction with H_2O in air [23].

The electrochemical performances of three types of Si were evaluated. Fig. 4(a) shows the first cycle voltage profiles in the range 0.01—2 V vs. Li/Li$^+$ at a current rate of 0.2 C. The first charge and discharge capacities of the sealed Si nanotube were 2924 and 2645 mAh g^{-1}, respectively, with the first coulombic efficiency of ~90%. After cap opening, the charge and discharge capacities decrease to 2000 and 1731 mAh g^{-1}, respectively. The cap-opened Si nanotubes electrode shows a slight decrease in the first coulombic efficiency (~85%) compared to that of sealed Si nanotubes. The coulombic efficiency of the cap-opened Si nanotubes is lower than the sealed Si nanotubes, which is related to the
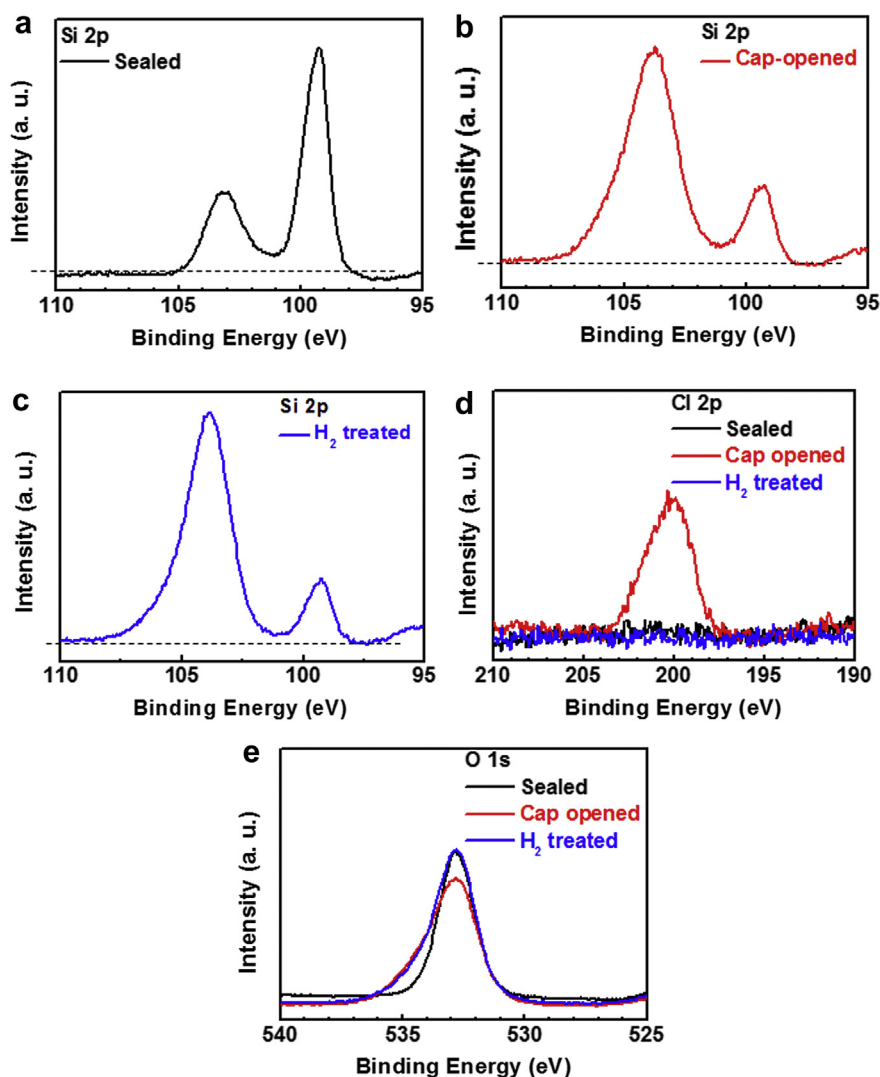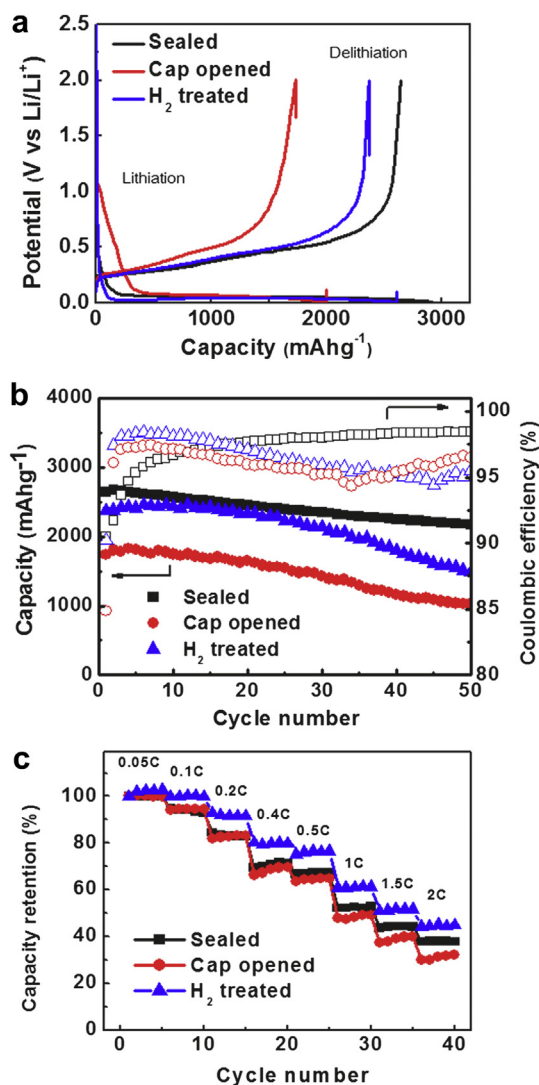

Fig. 3. Si 2p XPS spectra of (a) sealed Si nanotubes, (b) cap-opened Si nanotubes and (c) hydrogen treated, cap-opened Si nanotubes, (d) Cl 2p XPS spectra and (e) O 1s XPS spectra of Si nanotubes.

Fig. 4. Electrochemical performance of sealed Si nanotubes, cap-opened Si nanotubes, and hydrogen treated, cap-opened Si nanotubes. (a) Charge/discharge voltage profiles at a current rate of 0.2 C, (b) cycling performance and coulombic efficiency, and (c) rate capability (5 cycles were tested for each current density).

carried out to clarify this point. Cycling performances of sealed Si nanotubes and cap-opened Si nanotubes with and without hydrogen thermal treatment were also monitored for 50 cycles. The sealed Si nanotubes showed 2169 mAh g^{-1} and ∼81% of the specific capacity and capacity retention at 50 cycles, respectively. The cap-opened Si nanotubes yield lower capacity (1032 mAh g^{-1}) and capacity retention (∼60%). After hydrogen thermal treatment, there is a slight increase in the capacity (1486 mAh g^{-1}) and capacity retention (∼63%). After a few cycles, the sealed Si nanotubes electrode showed stable coulombic efficiency of more than 98% as shown in Fig. 4(b). Although our opened nanotube concept provided the general strategy to improve the rate capability of Si based anode, the issue on low coulombic efficiency should be addressed for the practical usage of Si based anode. On the contrary, the coulombic efficiencies of both cap-opened Si nanotube and hydrogen treated cap-opened Si nanotubes steadily decreased up to 95%. Although cap opened Si nanotube and hydrogen treated cap-opened Si nanotube structures showed lower cycle performances compared to that of sealed Si nanotubes, due to the accelerated electrolyte decomposition reactions through formation of solid electrolyte interface (SEI) films on large surface area, they exhibited improved rate capability performances.

The rate capabilities of Si nanotube anodes were evaluated at various current rates as shown in Fig. 4(c). The sealed Si nanotube and cap-opened Si nanotube yields similar rate performance. In striking contrast, the hydrogen treated cap-opened Si nanotubes electrode shows a slight increase (about 15%) in rate capability compared to both sealed and cap-opened Si nanotubes electrode. The discharge capacity yield of the sealed Si nanotube, cap-opened Si nanotube and hydrogen treated cap-opened Si nanotubes is found to be 52.3%, 48.2% and 61.1%, respectively, at a current rate of 1 C. Detailed sample information and their electrochemical performances are summarized in Table S1. The origin of the enhanced electrochemical kinetics for the hydrogen treated cap-opened Si nanotubes is closely related to its cap opened geometry, which allows 1) an increase in lithium ion flux due to enlarged interfacial area between active material and electrolyte 2) the decrease in lithium ion diffusion length due to the insertion of lithium ion through its inner and outer surface. It should be noted that, in the case of cap-opened Si nanotube, the degraded rate capability is attributed to the presence of lithium chloride acting as a blockage against lithium diffusion [16,17].

4. Conclusions

We demonstrated that the hydrogen treated, cap-opened Si nanotubes array is a promising anode structure for lithium ion battery exhibiting high rate capability. Opened nanotubes structure was simply synthesized from sealed Si nanotubes by RIE process using chlorine plasma. Hydrogen treated, cap-opened Si nanotubes geometry provides the shorter lithium diffusion length and higher lithium ion flux compared to those of the sealed Si nanotubes, which enables favorable lithium ion kinetics. Hydrogen treated, cap-opened Si nanotubes electrode shows a capacity of 61.1% at a current rate of 1 C, which is 15% higher than that of the sealed Si nanotubes electrode. Our cap-opening concept can be utilized in the preparation of other electrode materials to improve the rate capability of lithium ion battery.

undesirable side reaction for the formation of chloride compounds. However, after hydrogen thermal treatment, degraded capacities for the cap-opened Si nanotube are considerably recovered to 2615 and 2370 mAh g^{-1} for the first charge and discharge capacities, respectively. Especially, hydrogen treated, cap-opened Si nanotubes showed the initial coulombic efficiency of 90%, which is comparable with that of sealed Si nanotube. Although the SiO_x has lower specific capacity compared to that of Si, both the hydrogen treated, cap-opened Si nanotubes and the sealed Si nanotubes could have similar initial coulombic efficiency as the coulombic efficiency is the relative ratio between the charge capacity and the discharge capacity. It should be noted that SiO_x $(0 \leq X < 2)$ shows the different electrochemical performances, including specific capacity, coulombic efficiency and cycle performances, as a function of its stoichiometry [24–27]. The decrease in specific capacity of the cap-opened Si nanotubes and the hydrogen treated, cap-opened Si nanotubes was mainly attributed to increased SiO_x layer on the surface of Si nanotubes However, it is very difficult to obtain the mass ratio of Si/SiO_x and exact stoichiometry of SiO_x (native oxide layer) formed on the Si nanotube surface. Further study will be

Appendix A. Supplementary data

Supplementary data related to this article can be found at http://dx.doi.org/10.1016/j.jpowsour.2012.11.059.

References

[1] T. Song, J.L. Xia, J.H. Lee, D.H. Lee, M.S. Kwon, J.M. Choi, J. Wu, S.K. Doo, H. Chang, W. Il Park, D.S. Zang, H. Kim, Y.G. Huang, K.C. Hwang, J.A. Rogers, U. Paik, Nano Lett. 10 (2010) 1710.
[2] C.K. Chan, X.F. Zhang, Y. Cui, Nano Lett. 8 (2008) 307.
[3] C.K. Chan, H.L. Peng, G. Liu, K. McIlwrath, X.F. Zhang, R.A. Huggins, Y. Cui, Nat. Nanotechnol. 3 (2008) 31.
[4] Y. Idota, T. Kubota, A. Matsufuji, Y. Maekawa, T. Miyasaka, Science 276 (1997) 1395.
[5] B.A. Boukamp, G.C. Lesh, R.A. Huggins, J. Electrochem. Soc. 128 (1981) 725.
[6] L.B. Hu, H. Wu, S.S. Hong, L.F. Cui, J.R. McDonough, S. Bohy, Y. Cui, Chem. Commun. 47 (2011) 367.
[7] K.Q. Peng, J.S. Jie, W.J. Zhang, S.T. Lee, Appl. Phys. Lett. 93 (2008) 033105.
[8] H. Zhang, X. Yu, P.V. Braun, Nat. Nano 6 (2011) 277.
[9] C.C. Cheng, K.V. Guinn, V.M. Donnelly, I.P. Herman, J. Vac. Sci. Technol. A 12 (1994) 2630.
[10] N. Ozawa, T. Matsui, J. Kanamori, Jpn. J. Appl. Phys. 34 (1995) 6815. 1.
[11] K.H.A. Bogart, V.M. Donnelly, J. Appl. Phys. 87 (2000) 8351.
[12] R.D. Schnell, D. Rieger, A. Bogen, F.J. Himpsel, K. Wandelt, W. Steinmann, Phys. Rev. B 32 (1985) 8057.
[13] J. Matsuo, K. Karahashi, A. Sato, S. Hijiya, Jpn. J. Appl. Phys. 31 (1992) 2025. 1.
[14] T. Iimori, K. Hattori, K. Shudo, F. Komori, Surf. Sci. 437 (1999) 86.
[15] T. Takamura, K. Yoshimura, J. Suzuki, K. Sekine, J. Power Sources 174 (2007) 653.
[16] S.I. Pyun, S.B. Lee, E.J. Lee, Electrochim. Acta 47 (2001) 855.
[17] M. Aubay, E. Lojou, J. Electrochem. Soc. 141 (1994) 865.
[18] D.A. Zatsepin, P. Mack, A.E. Wright, B. Schmidt, H.J. Fitting, Phys. Status Solidi A 208 (2011) 1658.
[19] F.J. Himpsel, F.R. Mcfeely, A. Talebibrahimi, J.A. Yarmoff, G. Hollinger, Phys. Rev. B 38 (1988) 6084.
[20] N. Layadi, V.M. Donnelly, J.T.C. Lee, J. Appl. Phys. 81 (1997) 6738.
[21] E. Paparazzo, M. Fanfoni, E. Severini, S. Priori, J. Vac. Sci. Technol. A 10 (1992) 2892.
[22] M.E. Simonsen, C. Sonderby, Z.S. Li, E.G. Sogaard, J. Mater. Sci. 44 (2009) 2079.
[23] M.L. Wise, O. Sneh, L.A. Okada, S.M. George, Surf. Sci. 364 (1996) 367.
[24] W.-S. Chang, C.-M. Park, J.-H. Kim, Y.-U. Kim, G. Jeong, H.-J. Sohn, Energy Environ. Sci. 5 (2012) 6895–6899.
[25] C.M. Park, W. Choi, Y. Hwa, J.H. Kim, G. Jeong, H.J. Sohn, J. Mater. Chem. 20 (2010) 4854–4860.
[26] J.I. Lee, N.S. Choi, S. Park, Energy Environ. Sci. 5 (2012) 7878–7882.
[27] T. Zhang, J. Gao, H.P. Zhang, L.C. Yang, Y.P. Wu, H.Q. Wu, Electrochem. Commun. 9 (2007) 886–890.